


Phenomenological modeling of combustion and NO_x emissions using detailed tabulated chemistry methods in diesel engines

International J of Engine Research
2016, Vol. 17(8) 846–856
© IMechE 2015
Reprints and permissions:
sagepub.co.uk/journalsPermissions.nav
DOI: 10.1177/1468087415619302
jer.sagepub.com


Reza Rezaei¹, Friedrich Dinkelacker², Benjamin Tilch¹,
Thaddaeus Delebinski¹ and Maximilian Brauer¹

Abstract

Enhancing the predictive quality of engine models, while maintaining an affordable computational cost, is of great importance. In this study, a phenomenological combustion and a tabulated NO_x model, focusing on efficient modeling and improvement of computational effort, is presented. The proposed approach employs physical and chemical sub-models for local processes such as injection, spray formation, ignition, combustion, and NO_x formation, being based on detailed tabulated chemistry methods. The applied combustion model accounts for the turbulence-controlled as well as the chemistry-controlled combustion. The phenomenological combustion model is first assessed for passenger car application, especially with multiple pilot injections and high exhaust gas recirculation ratios for low-load operating points. The validation results are presented for representative operating conditions from a single-cylinder light-duty diesel engine and over the entire engine map of a heavy-duty diesel engine. In the second part of this study, a novel approach for accurate and very fast modeling of NO formation in combustion engines is proposed. The major focus of this study is on the development of a very fast-running NO mechanism for usage in the next generation of the engine control units. This approach is based on tabulation of a detailed chemical kinetic mechanism and is validated against the detailed chemical reaction mechanism at all engine-relevant conditions with the variation in pressure, temperature, and air–fuel ratio under stationary and ramp-type transient conditions in a perfectly stirred reactor. Using this approach, a very good match to the results from calculations with the detailed chemical mechanism is observed. Finally, the tabulated NO_x kinetic model is implemented in the combustion model for in-cylinder NO_x prediction and compared with the experimental engine measurement data.

Keywords

Diesel engine, combustion, phenomenological modeling, NO_x emissions, reaction kinetics

Date received: 11 June 2015; accepted: 27 October 2015

Introduction

Numerical simulation methods are utilized as a standard tool for the description of internal combustion engine processes and for the optimization to fulfill future emission standards, fuel consumption reduction, and improved safety and drivability, see for example, Heywood.¹ A predictive model that accounts for several engine processes such as combustion and emission formation plays a decisive role in powertrain development, including optimization of engine components as well as development, testing, and model-based calibration of combustion and aftertreatment control strategies.²

Fast empirical combustion models, for example, Vibe function,³ often suffer from a lack of

predictability. Phenomenological models have the advantage of being both easy to handle and computationally efficient. In addition, they are capable of predicting several effects of important parameters on the combustion process and emission formation.

In recent years, multiple modeling approaches have been studied by various investigators. For instance, the

¹IAV GmbH, Gifhorn, Germany

²Institute for Technical Combustion, Leibniz University of Hannover, Hannover, Germany

Corresponding author:

Reza Rezaei, IAV GmbH, Nordhoffstr. 5, Gifhorn 38518, Germany.
Email: reza.rezaei@iav.de

approach proposed by Chmela et al.^{4,5} is a global model based on a single-zone description of the combustion chamber. It does not require subdividing of the combustion chamber into zones of different compositions and temperatures. Therefore, it offers a fast and computationally efficient modeling. This is categorized as a phenomenological combustion model, since it relates the burning rate to the engine characteristic parameters (e.g. the injection rate as a time-dependent input parameter).^{6,7} The main issue of this model is the hypothesis that the rate of fuel combustion is determined by the rate of air–fuel mixing. The rate of air–fuel mixing depends on the injection rate as well as turbulent kinetic energy.

More detailed models are generally less computationally efficient. For example, the so-called packet model from Hiroyasu et al.^{8,9} can be mentioned, in which the compression stroke is modeled with one zone, while the injection spray is discretized into small packets in axial and radial directions. Other authors follow this concept, for example, Gao and Schreiber,¹⁰ Morel and Wahiduzzaman,¹¹ and Stiesch and Merker.¹² Stiesch and Merker¹² modified this model so that the maximum burning rate of each packet depends not only on the vaporized fuel and the available air but also on the maximum chemical reaction rate. Barba et al.⁷ proposed an empirical and a phenomenological combustion model. The phenomenological combustion model accounts for premixed as well as the diffusion combustion in combination with an ignition delay model.

The multi-zone models are an efficient alternative to the computationally intensive three-dimensional (3D) simulation of in-cylinder flow, mixture formation, and detailed chemistry in each cell. A hybrid procedure using fluid mechanics code KIVA and a detailed chemical kinetics is used by Aceves et al.¹³ to capture the temperature gradients inside the cylinder for homogeneous charge compression ignition (HCCI) combustion.

A fully coupled multi-zone model is presented by Babajimopoulos et al.¹⁴ The multi-zone model communicates with KIVA-3V at each computational time step. Therefore, essential information about mixture preparation and combustion progress from each computational cell are considered by the multi-zone methodology. The multi-zone solution from the detailed mechanism is then remapped to the 3D grid. A good agreement to the detailed solution is observed. Performing detailed chemistry calculation for relatively small number of zones reduces the computational effort in comparison to the case, resolving all computational cells.

In order to include other cell variables, such as mass fraction of each species, an improvement of the zoning strategy and its performance is given by Raju et al.¹⁵ Furthermore, two remapping techniques are evaluated. Test cases with gasoline and diesel engine simulations are performed with different exhaust gas recirculation (EGR) scenarios.

Combustion model formulation

As the focus of this study is set on highly efficient modeling of combustion, the approach of Chmela et al.⁵ for single-zone modeling of spray and combustion is used as the basis of the development. The fuel spray is not modeled with the packet approach. The time evolution of spray characteristics is governed by mass and momentum conservation equation of the spray control volume. The model is integrated as a user subroutine in the simulation software GT-Power¹⁶ accounting for two-zone description of the cylinder thermodynamics. The working fluid consists of an unburned zone and a burned zone with energy and mass interactions between themselves. For each zone, the thermodynamic properties such as temperature and gas composition are calculated separately.

The injection rates are the experimentally measured data at the IAV hydraulic test bench and used for calibration of the phenomenological nozzle model of Von Kuensberg Sarre et al.¹⁷ This phenomenological nozzle flow model considers the nozzle passage inlet configuration to calculate the nozzle discharge coefficient and injection pressure at the nozzle hole as well as the cone angle and the effective injection velocity for a given injection rate.

In terms of turbulence modeling, two sources of turbulence production, especially for passenger car engines, are considered. The first source is the kinetic energy of the inlet flow generated through intake ports as swirl or tumble motion during the intake phase. Another formulation is proposed for the squish flow resulting from piston movement as an important production source near top dead center. Computational fluid dynamics (CFD) simulations of intake and compression phase show that the contribution of first two sources in the total amount of turbulent kinetic energy is considerable.¹⁸

For brevity, only the highlights of the combustion model for modeling the multiple pilot injections for passenger car application are presented here. More detail about the physical sub-models such as injection, spray formation, and combustion can be found in Rezaei et al.¹⁸

Ignition model

The applied ignition model employs semi-empirical models for both physical and chemical sub-processes accounting for ignition delay. Modeling of the chemical ignition delay is performed by a least-square fitted ignition model of Weisser¹⁹ for *n*-heptane ignition that enables the capture of the low-temperature and high-temperature ignition behavior, including the negative temperature coefficient (NTC) region in between (Figure 1). In order to consider the effect of physical sub-processes on ignition delay, a simple formulation used by Barba et al.⁷ is used to describe the physical ignition delay.

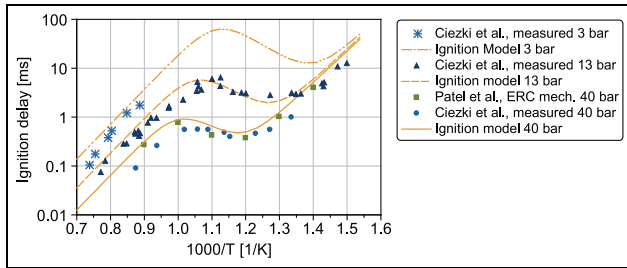


Figure 1. Comparison of the ignition delay sub-model with experimental measurements of Ciezki and Adomeit²⁰ and the reduced reaction kinetic mechanism of Patel et al.²¹

Premixed and diffusion combustion modeling

The combustion model is principally a laminar-and-turbulent characteristic time combustion model which is frequently used in CFD models for diesel engine combustion²² with improvements accounting for the premixed, diffusion, and burn-out combustion.¹⁸ This handles the two extremes of combustion, reactions limited by kinetics and those limited by mixing.

For the reaction kinetics limit, the time rate of change for species i is used as by Kong et al.²² given by

$$\frac{\partial \tilde{Y}_i}{\partial t} = - \frac{\tilde{Y}_i - \tilde{Y}_i^*}{\tau_{chem}} \quad (1)$$

where \tilde{Y}_i is the mass fraction and \tilde{Y}_i^* is the thermodynamic equilibrium value of the mass fraction for species i . Here, τ_{chem} is a characteristic time scale to achieve the equilibrium. The equilibrium concentration of fuel is taken equal to 0.²² With these assumptions, Kong et al.²² combined equation (1) with the correlated one-step reaction rate from a single droplet autoignition experiment²³ and derived the laminar time scale as

$$\tau_l = A [fuel]^{0.75} [O_2]^{-1.5} \exp\left(\frac{E}{RT}\right) \quad (2)$$

The activation energy is taken as $E = 77.3$ kJ/mol considering tetradecane. The parameter A is used here as a calibration parameter to be adapted for each engine configuration. The effects of EGR and oxygen concentration as well as fuel concentration in the mixture are taken into account.

Combustion limited by mixing is the other extreme, if the chemical time scales are negligibly small compared to the turbulent mixing time scales. For instance, the Eddy break-up (EBU) model assumes the resulting effective reaction rate to be proportional to the reciprocal of the turbulent time scale.²⁴ In fact, the entire spectrum of combustion regimes can be found in diesel engine combustion. This means that at any time there may be a partial burning in either a kinetically limited or mixing-limited way, while the overall combustion often lies somewhere in between these extremes. The

Table 1. Specifications of the passenger car single-cylinder test engine.

| | |
|----------------------------|-------------------------------------|
| Bore | 83 mm |
| Stroke | 99 mm |
| Compression ratio | 16.2 |
| Max. peak firing pressure | 220 bar |
| Number of nozzle holes | 8 |
| Nozzle hydraulic flow rate | 710 cm ³ /min at 100 bar |

developed combustion model accounts for both laminar and turbulent time scales.

For passenger car applications, there are considerable amount of low-load points in the engine map which are operated in the New European Driving Cycle (NEDC). These points may have moderate or high EGR rates with multiple pilot injections, and therefore, a major portion of the combustion is premixed and chemically controlled. The combustion model is improved here in order to calculate the ignition delay considering the low temperature, NTC ignition, and the high-temperature ignition which may happen by an early pilot injection, late main, or a post injection. The ignition delay is calculated for each injection event. The spray model calculates the mixture preparation for each event individually. The effect of air-entrainment and dilution of mixture before and after combustion has an important effect on ignition and premixed combustion afterward. This is considered in the spray model, providing the mass fraction of the mixed fuel above a certain relative air-fuel ratio as a function of mixing time, and this crucial input is used by the combustion model for each injection event separately.

Test engines

The combustion model is validated using measurement data of different diesel engines, from passenger car up to heavy-duty applications, utilizing EGR and various injection strategies. For brevity, only two validation engines are presented here.

Light-duty passenger car diesel engine

The presented combustion model is modified for passenger car light-duty application with relatively high EGR ratios and multiple pilot injections with focus on part- and low-load cases which are relevant for the European exhaust-emission legislation in the NEDC cycle. The thermodynamic measurements are conducted on a passenger car single-cylinder engine with a displacement of approximately 536 cm³. The engine has a common-rail injection system equipped with an eight-hole nozzle. All relevant pressures and temperatures (intake air, EGR, exhaust gas, lubricant, coolant) are controlled externally by the test bench. The main engine parameters are listed in Table 1:

Table 2. Investigated operating points using the passenger car single-cylinder engine.

| Operating point | Engine speed (l/min) | Mean effective pressure (bar) | Rail pressure (bar) | EGR rate (%) | SOI (°CA ATDC) |
|-----------------|----------------------|-------------------------------|---------------------|--------------|----------------------------|
| A | 3700 | 14.9–17.4 | 1600–2200 | 0 | −13.7 |
| B | 1200 | 6.2–6.5 | 800 | 34–38 | −6.8, −9.2, −11.4, −14.0 |
| C | 1200 | 6.2–6.3 | 800 | 0–41 | −12.6, −13.6, −14.0, −14.2 |

EGR: exhaust gas recirculation; SOI: start of injection; CA: crank angle; ATDC: after top dead center.

Heavy-duty diesel engine

The second validation engine is a heavy-duty diesel engine, certified for the non-road Tier 4i emission standard. It has a displacement of approximately 2000 cm³ for each cylinder and a common-rail injection system equipped with an eight-hole nozzle. No EGR is applied at this engine. All points on the engine map are considered (Figure 2).

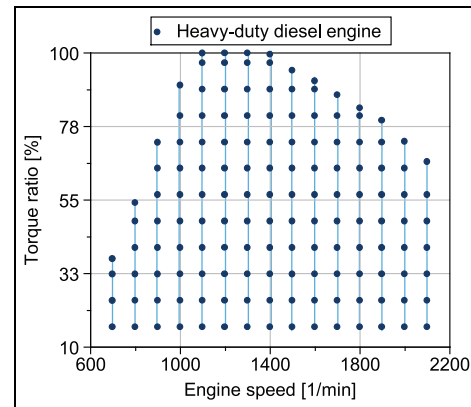


Figure 2. Investigated engine operating points of the heavy-duty diesel engine.

Validation of the phenomenological combustion model

Light-duty passenger car diesel engine

For the light-duty passenger car engine, at first, a full-load operating point is selected for validation of the combustion model with variation of the rail pressure. For the two part-load operating points, a start of injection (SOI) variation and an EGR variation are carried out. As given in Table 2, the engine speed differs for the part- and full-load cases. GT-Power is used as simulation platform and the integrated combustion model is

used for modeling of heat release rate with the same parameters for all operating points.

Figure 3 compares the simulated in-cylinder pressure with the measurement. Shifting the SOI to an earlier time increases the maximum cylinder pressure and the

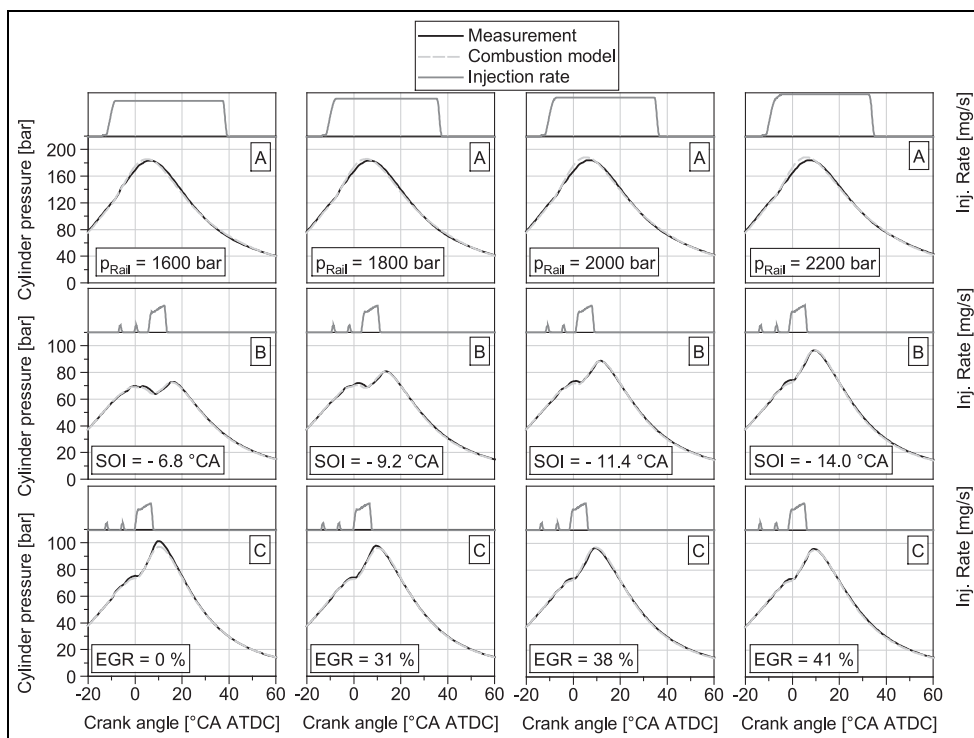


Figure 3. Comparison of the simulated in-cylinder pressure with measurement. Operating points A, B, and C correspond to n = 3700, 1200, and 1200 l/min.

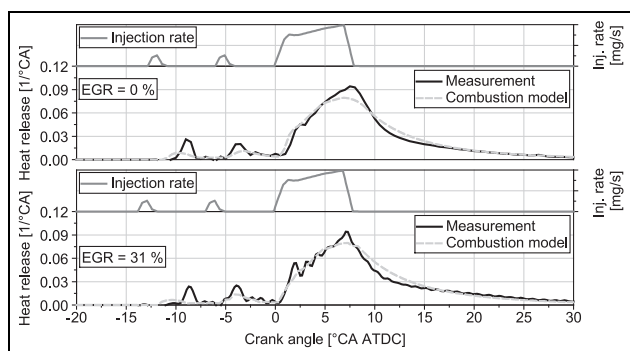


Figure 4. Heat release rate obtained from the combustion model and thermodynamic analysis of experimental results. Operating point C corresponds to $n = 1200$ 1/min.

pressure gradient, which are both reproduced properly by simulation. A good match is observed between simulation and measurement in Figure 3.

A comparison between the heat release rate obtained from a thermodynamic analysis of the measured cylinder pressure and the simulated heat release rate is plotted in Figure 4. For a better illustration, only two points from the low-load operating point, with no EGR and a high EGR rate, bottom-left of Figure 3 (0% and 31%), are selected. The observed small deviations in the heat release rate result in minor deviations in cylinder pressure accounting for the design target of the modeling, for example, focusing on engine power or fuel consumption (Figure 4). Overall, a good match between simulation and measurement is observed.

Heavy-duty diesel engine

Additionally, the phenomenological combustion model is investigated on a heavy-duty diesel engine. Calibration of the combustion model parameters is carried out for nine representative operating points and then used with the same parameters for the entire engine map.

Three important engine speeds of 1200, 1500, and 1900 1/min with engine load of 25%, 50%, 75%, and 100% are selected for plotting in Figure 5. For brevity, only the simulated heat release rate is compared with the results obtained from the thermodynamic analysis of the measured cylinder pressure. A good concordance between simulation and measurement is obtained for all the full- and part-load cases.

Tabulated NO_x kinetic model

The emission of nitrogen oxides (NO_x) is a challenge for internal combustion engines. The formation of NO or NO_2 is determined by complex chemical processes, being strongly dependent on the temperature. A fast and efficient prediction of the NO_x emissions depending on the engine parameters is therefore a

rather difficult task. Thermal equilibrium calculations are the first approximation, but are commonly known to be insufficient. In the following work, this is compared with three other approaches: the extended Zeldovich mechanism; a fully detailed reaction mechanism which, however, is much too slow for in situ calculations; and a newly developed combined method of a tabulation and a relaxation procedure, being very fast.

The extended Zeldovich mechanism²⁵ is a common reaction kinetic mechanism to model the thermal NO formation and is often used in one-dimensional (1D) as well as three-dimensional (3D) simulation tools, employing three kinetic reactions and assuming further equilibrium reactions. These equilibrium reactions are required to calculate the H, O, and OH radicals for the three slower kinetic reactions, determining the NO concentration. The Zeldovich mechanism is especially relevant at high temperatures ($T > 1700$ K), where the hydrogen and oxygen radicals dominate a series of NO-forming reactions. Further routes are the prompt NO_x formation, the path via NNH or via nitrous oxides.^{26,27} These routes can be calculated with detailed reaction mechanisms, for instance, the GRI-Mech 3.0²⁸ mechanism. Although reaching commonly predictive results, this approach would need by far too much computational effort, to be applied in very fast applications such as in on-board engine control units (ECUs). In this study, therefore, another approach is developed, combining the detailed chemistry with a tabulation method and the most essential temporal behavior with a relaxation method. For that, first, an analytical investigation of NO_x formation kinetics in all engine-relevant conditions is carried out, using the detailed chemical reaction mechanism GRI-Mech 3.0 with 325 reactions and 53 species.²⁸ Figure 6 shows the investigated operating conditions from 2000 to 3000 K as well as various relative air–fuel ratios from 0.7 to 3.0. Each of these operating conditions is simulated in a perfectly stirred and adiabatic reactor with the full detailed reaction mechanism. The reactor pressure and temperature are defined as constant values at the start of the simulation. The mole fraction of each species, O, H, OH, and so on, is initialized equal to its mole fraction in the equilibrium state by the given pressure, temperature, and air–fuel ratio, assuming that combustion is very fast compared to the NO formation kinetic and the combustion products are in equilibrium state at the start of the reactor simulation. These initialized values at the equilibrium state are calculated by the detailed GRI-Mech 3.0. NO is initialized as zero and is formed in this perfectly stirred reactor until reaching its value at the equilibrium condition.

For comparison, also the simpler Zeldovich mechanism is calculated. The rate constants of the Zeldovich mechanism are used as given by Bowman.²⁹ The same initial conditions such as temperature, pressure, and species concentration are implied for both the detailed kinetic model and Zeldovich mechanism at the start of

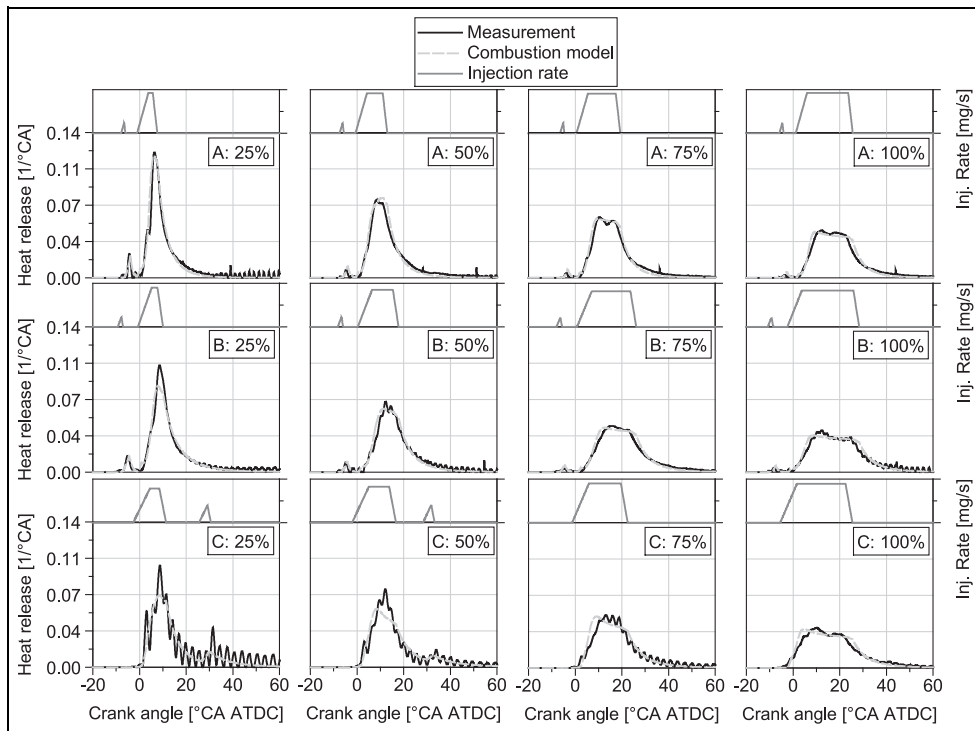


Figure 5. Heat release rate obtained from the combustion model and thermodynamic analysis of experimental investigation. Operating points A, B, and C correspond to $n = 1200, 1500,$ and 1900 l/min with 25%, 50%, 75%, and 100% load.

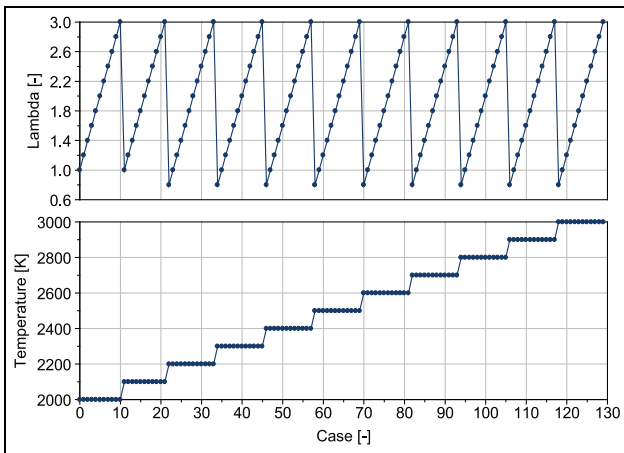


Figure 6. Temperature and pressure variation for each reactor simulation case.

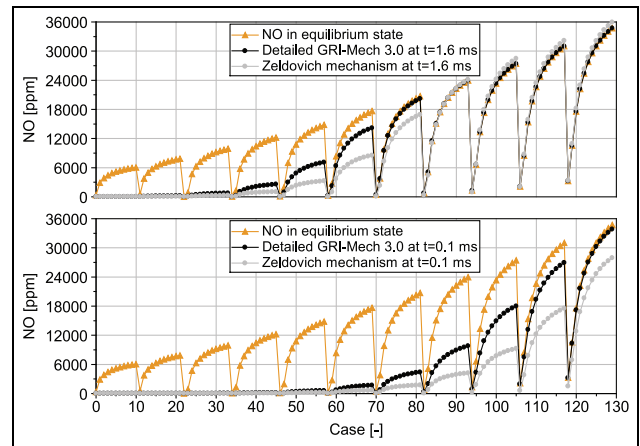


Figure 7. Comparison of the NO concentration in a perfectly stirred reactor at 0.1 and 1.6 ms after start of NO formation for various operating conditions.

reactor simulation. In order to evaluate the Zeldovich mechanism, NO concentrations at the different representative times after the start of NO formation are compared with the values obtained from the detailed kinetic model as well as their values in the equilibrium condition (Figure 7).

The selected post-processing time of 1.6 ms in Figure 7 corresponds to, for example, 12° CA at 1250 l/min, which is an important time scale for combustion and emission formation. As Figure 7 illustrates, large deviation between the calculated NO by the Zeldovich mechanism and the detailed GRI-Mech 3.0

mechanism is observed during the formation phase. Depending on the operating conditions and completeness of NO formation, an inaccuracy factor of about approximately 2 is observed in the formation phase. This correlates with an uncertainty factor of 2 for NO formation reactions.¹

It can be concluded here that the Zeldovich mechanism with a big deviation in prediction of the NO formation phase could be a source of inaccuracy in simulation of NO_x emissions in combustion engines. However, a direct implementation of a detailed reaction mechanism such as GRI-Mech 3.0 or even a

reduced mechanism with fewer reactions as proposed, for example, by Yoshikawa and Reitz,³⁰ is computationally not affordable for a fast-running phenomenological combustion model.

For improving the accuracy and computational time, a tabulated chemistry method for modeling the NO formation, based on the characteristic chemical relaxation time scale, is proposed. This is similar to the proposed model of Kong et al.²² for modeling the premixed combustion

$$\frac{\partial \tilde{Y}_i}{\partial t} = -\frac{\tilde{Y}_i - \tilde{Y}_i^*}{\tau_{chem}} \quad (3)$$

Here, for NO formation, τ_{chem} is taken as the characteristic formation time scale and \tilde{Y}_i^* as the NO concentration in the equilibrium state. Solving the above differential equation with the initial conditions of $NO(t=0) = 0.0$ leads to

$$NO(t) = NO^* - NO^* e^{-\frac{t}{\tau_{chem}}} \quad (4)$$

In order to calculate the NO concentration using equation (4), the characteristic chemical time, τ_{chem} , and the NO concentration in equilibrium condition, NO^* , are required. These values can be calculated from the GRI-Mech 3.0 detailed chemical reaction mechanism in a perfectly stirred reactor for various temperatures and air–fuel ratios and are provided as look-up tables. A temperature range from 2000 to 3000 K and different gas compositions according to the relative air–fuel ratios from 0.4 to 3.0 at a constant pressure of 80 bar are selected for tabulation of the required parameters.

Calibration of the proposed reaction mechanism and calculation of both parameters for each simulation case are performed by minimization of error using the particle swarm optimization solver.³¹ Figure 8 compares the NO formation at 80 bar and temperature of 2700 K for different relative air–fuel ratios.

A very good match between the proposed NO_x kinetic model and the results obtained from the detailed GRI-Mech 3.0 mechanism with 325 reactions and 35 species is obtained. In order to assess the accuracy of the proposed kinetic mechanism, the deviation from the simulated NO by the detailed mechanism during the formation phase is calculated and the relative error (in %) is given by equation (5)

$$\text{Relative error} = \frac{\int_0^{t_{equil.}} |NO_{Tab. Model}(t) - NO_{Detailed mech.}(t)| dt}{\int_0^{t_{equil.}} NO_{Detailed mech.}(t) dt} \cdot 100\% \quad (5)$$

Figure 9, right side, shows that the relative error for the majority of simulated cases is lower than 1%. For some points with low temperature and rich mixture, a higher relative error is observed; however, as shown at

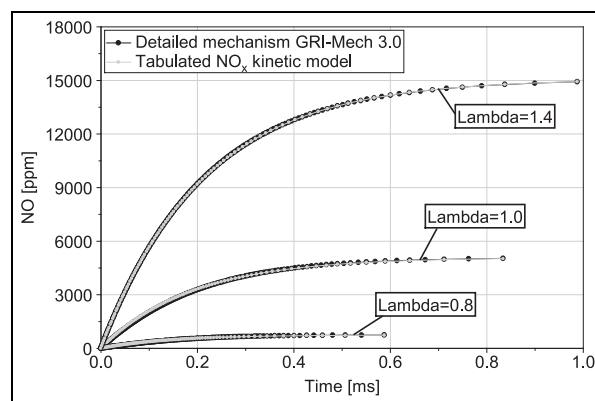


Figure 8. Validation of the tabulated NO_x kinetic model for NO formation in a perfectly stirred reactor at 2700 K and 80 bar for different relative air–fuel ratios.

the left side of Figure 9, the NO concentration for this region is about 5–10 ppm, so overall a very good match is reached. With this very fast modeling approach, neither kinetics nor equilibrium reactions need to be solved. Consequently, the computational speed is significantly improved without loss in accuracy which enables this approach even for ECU applications.

An important parameter which is investigated in this study is the effect of NO concentration at the start of the reactor simulation on the chemical time constant. In engine simulation, in the early phase of combustion with relatively high temperature, NO is formed in the burned zone and in the later phase of combustion, because of fast mixing with the unburned mixture, the temperature is reduced. Therefore, it may happen that the local concentration of NO is higher than the NO concentration in the equilibrium condition of the corresponding temperature and thus a backward reaction occurs.

In order to evaluate the ability of the proposed kinetic mechanism in such conditions, all the mentioned operating conditions, temperature, and air–fuel ratio variations are simulated with a start value of NO concentration equal to the NO concentration of the corresponding equilibrium conditions plus 2000 ppm. Principally, this starting value does not change the characteristic time scale. However, with a starting value far from the concentration in the equilibrium condition, a more accurate fitting can be achieved. Because until reaching the equilibrium conditions, more points during a longer time are considered. Practically, for the cases with a starting value lower than the equilibrium concentration, the starting value is set to 0 and for the case having NO more than in the equilibrium concentration, the NO concentration of the corresponding equilibrium conditions plus 2000 ppm is selected, as the start value.

It is observed that a modification of the chemical reaction time scale is necessary. In order to reach the best match, the chemical time can be given as an additional look-up table or be correlated as

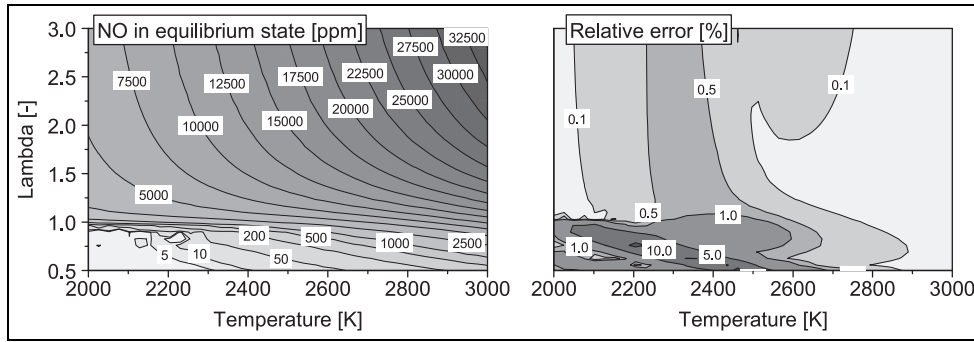


Figure 9. Evaluation of the tabulated NO_x kinetic model for NO formation in a perfectly stirred reactor at various temperatures and air–fuel ratios.

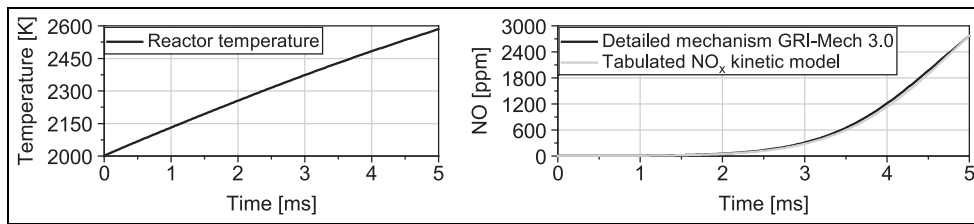


Figure 10. Evaluation of the tabulated NO_x kinetic model for NO formation in a perfectly stirred reactor and a transient temperature ramp.

$$\begin{aligned} \tau_{2000\text{ppm}}(T, \lambda) &= (C_T \cdot T + C_\lambda \cdot \lambda + C) \cdot \tau_{0\text{ppm}} \\ C_T &= 5.568E - 4, C_\lambda = 7.599E - 2, \\ &\text{and } C = -5.337E - 1 \end{aligned} \quad (6)$$

where $\tau_{0\text{ppm}}$ is the chemical time scale for calculation of NO concentration when the instantaneous value of NO concentration is lower than the equilibrium value of NO by the corresponding temperature and air–fuel ratio; otherwise, the correlated time scale, $\tau_{2000\text{ppm}}$, can be used.

In order to reduce the amount of tabulated data and increase the computational speed, only one constant pressure of 80 bar is considered and the effect of the reactor pressure is treated as the next step. A variation in the reactor pressure from 80 to 200 bar is carried out for all the above-mentioned temperatures and air–fuel ratios. It is observed from the pressure variation that the value of the NO in equilibrium condition does not change significantly with the pressure. But for the characteristic chemical time scale, a simple correlation for considering of the effect of pressure is proposed in equation (7)

$$\tau(p) = \begin{cases} 15.4196 \cdot p^{-0.5538} \cdot \tau_{140\text{bar}}; & T \geq 2400 \text{ K}, \lambda > 1 \\ 22.3089 \cdot p^{-0.6285} \cdot \tau_{140\text{bar}}; & T < 2400 \text{ K}, \lambda > 1 \end{cases} \quad (7)$$

The best correlation for the pressure variation from 80 to 200 bar is obtained if 140 bar is taken as the basis pressure. For brevity, the deviation analysis is not plotted for all the investigated pressures. When using

equation (7), the average error is lower than 1% for each pressure, considering all temperatures and air–fuel ratios.

All the above-mentioned investigations are carried out with stationary reactor simulation. Evaluation of the developed kinetic model in transient conditions is performed, first, in a perfectly stirred reactor with a ramp-type temperature increase. Figure 10 illustrates the temperature ramp in the reactor and compares the NO concentration from the proposed kinetic mechanism, to the simulated value using the detailed mechanism. The calculated NO in the reactor by the tabulated kinetic model correlates well with the results of the detailed mechanism.

As the final step for evaluation of the developed reaction kinetic model, the calculated NO_x emissions are compared with the results from the detailed GRI-Mech 3.0 mechanism under different engine operating points. Both GRI-Mech 3.0 and the developed NO_x kinetic model are coupled with the same combustion model and two-zone temperature model for calculating the burned and unburned temperatures. Figure 11 compares the NO_x calculated by the detailed mechanism with the results obtained from the tabulated kinetic model for different engine speeds of the heavy-duty engine with 55% load.

As depicted in Figure 11, a very good match between the NO_x calculated by the detailed mechanism and the proposed kinetic mechanism with a transient variation in the temperature, pressure, and air–fuel ratio in the burned zone under real-engine operating conditions for various engine speeds is obtained.

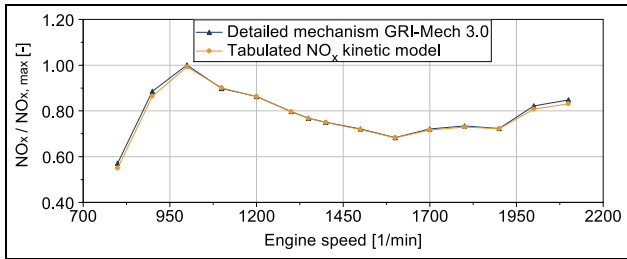


Figure 11. Comparison of the simulated NO_x emissions by the detailed GRI-Mech 3.0 mechanism and the tabulated kinetic model for the heavy-duty engine with 55% load.

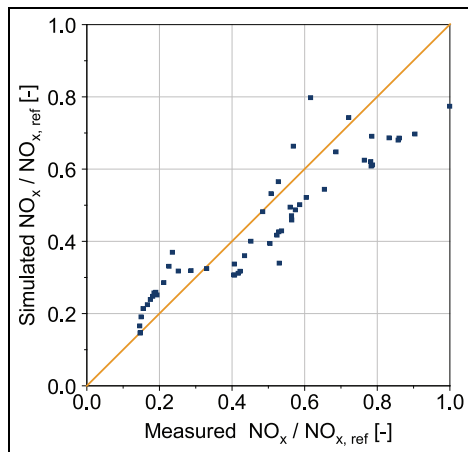


Figure 12. Comparison of NO_x emissions for the heavy-duty engine in overall engine operating points with measurement results.

Finally, the tabulated NO_x kinetic model is implemented in the phenomenological combustion model. Both NO_x and combustion models are coupled to the GT-Power software for simulation of combustion and in-cylinder NO_x emissions. The combustion model calculates the burning rate, and the NO_x model, with the new kinetic mechanism, calculates the NO_x in the burned zone. Calculation of the burned zone temperature is simply based on the two-zone modeling approach commonly used in computationally efficient phenomenological models. Figure 12 illustrates the calculated and measured NO_x emissions obtained from the new NO_x kinetic model, coupled with the above-mentioned phenomenological combustion model for the heavy-duty diesel engine. The operating points shown in Figure 2 with the torque ratio above 20% are selected. Both the simulated and measured NO_x emissions are normalized by the same reference value. A relatively good match between the measured and simulated NO_x is obtained.

It should be noted that an accurate calculation of in-cylinder NO_x emissions strongly depends on the calculation of the burned zone temperature and the mixing rate between the burned and unburned zone. The crucial information about spray formation, turbulent kinetic energy, ignition delay, and distribution of the

air-fuel mixture in the combustion chamber can be provided by a phenomenological combustion model, which enhances the accuracy of temperature calculation and consequently the predictability of the NO_x model. However, the focus of this study is the development of an improved NO_x kinetic mechanism. Further improvement of the two-zone mixing model with the help of the combustion model is a focus of future works. An analysis of engine NO_x emissions for the light-duty passenger car engine is not performed.

As mentioned before, one motivation for developing phenomenological combustion model and the NO_x kinetic mechanism is the improvement of the model accuracy for 1D engine process simulation. Besides the model accuracy, the computational time is an important factor. The presented engine process simulation for the heavy-duty application runs with about factor 2 slower than the real time on a PC with 1.8 GHz processor using the GT-Power software.

In comparison to the Zeldovich mechanism, the proposed NO_x calculation approach reduces the computational time significantly, which enables it as the best model for usage in the next generation of ECUs. However, as mentioned before, the NO_x model requires the information on combustion and burn rate which can be ideally delivered by the combustion model.

The authors are working on optimization of the presented combustion model, enabling it running in an ECU, not only for NO_x prediction but also for combustion control. Developing a very fast-running combustion model to run in ECU, for combustion control and in conjunction with the NO_x model as the future concept, seems to be feasible for the authors.

Another possibility for using the developed NO_x kinetic mechanism in the ECU is in conjunction with the cylinder pressure sensor. The cylinder pressure sensor is in series production by some car manufactures such as Volkswagen.³² A thermodynamic analysis of the cylinder pressure is also implemented in the ECU.³² The thermodynamic analysis from the measured cylinder pressure delivers heat release rate as well as the temperature of the burned zone. Principally, with this information, the NO_x emissions can be calculated.³³ However, using a predictive combustion model, the predictive ability of the NO_x model can be significantly improved, when essential information about injection, mixture preparation, ignition, and combustion are physically calculated and delivered by a predictive combustion model.

Conclusion

A phenomenological combustion model with a novel NO_x reaction kinetic model has been developed. The combustion model exhibits a good predictability for different combustion systems and engine sizes from passenger car to heavy-duty diesel engines, under different operating conditions. The combustion model has a high

computational speed and can provide a good platform for evaluation of control strategies as well as engine transient cycles when integrated in the simulation software GT-Power. This study is especially focused on model simplification and thereby reduction in the computational effort. This enables an implementation of such physical-based models as a platform for combustion control and emission calculation in the next generation of the ECUs.

The tabulated kinetic model enables fast execution as it relies on a single equation and does not require any equilibrium reaction for NO calculation. This enables the model to be used in a detailed 3D CFD simulation or even for NO_x calculation in ECUs with low computational capacity. The proposed NO_x kinetic model shows very good accuracy in comparison with the detailed GRI-Mech 3.0 mechanism in stationary as well as in transient conditions in a perfectly stirred reactor and also in combination with the phenomenological combustion model under real-engine operating conditions. The phenomenological combustion model with sub-models dealing with in-cylinder processes from injection to combustion delivers essential information on mixture formation and burning rate in order to improve the in-cylinder NO_x prediction.

Acknowledgements

The authors would like to thank colleagues at IAV GmbH, Mrs H. Puschmann, Mr E. Neumann, and Mr J. Seebode as well as Mr K. Kuppa from the Institute for Technical Combustion at the University of Hannover, for their valuable help and technical support.

Declaration of conflicting interests

The author(s) declared no potential conflicts of interest with respect to the research, authorship, and/or publication of this article.

Funding

The author(s) received no financial support for the research, authorship, and/or publication of this article.

References

- Heywood JB. *Internal combustion engine fundamentals*. New York: McGraw-Hill, 1988.
- Bertram C, Rezaei R, Tilch B and van Horrick P. Development of an Euro VI engine using model-based calibration. *MTZ Worldw* 2014; 75(10): 4–9.
- Vibe I. *Brennverlauf und Kreisprozess von Verbrennungsmotoren*. Berlin: VEB Verlag Technik, 1970.
- Chmela F, Pirker G and Wimmer A. Zero-dimensional ROHR simulation for DI diesel engines—a generic approach. *J Energy Convers Manag* 2007; 48: 2942–2950.
- Chmela F, Pirker G, Losonczi B, Wimmer A, Desantes J and García-Oliver J. A new burn rate simulation model for improved prediction of multiple injection effects on large diesel engines. In: *Thiesel conference*, Valencia, 14–17 September 2010. Valencia: Universidad Politècnica de València.
- Stiesch G. *Modeling engine spray and combustion processes*. Berlin: Springer-Verlag, 2003.
- Barba C, Burkhardt C, Boulouchos K and Bargende M. A phenomenological combustion model for heat release rate prediction in high-speed DI diesel engines with common rail injection. SAE paper 2000-01-2933, 2000.
- Hiroyasu H, Kadota T and Arai M. Development and use of a spray combustion modeling to predict diesel engine efficiency and pollutant emission. Part 1: combustion modeling. *Bull JSME* 1983; 26: 569–575.
- Hiroyasu H, Kadota T and Arai M. Development and use of a spray combustion modeling to predict diesel engine efficiency and pollutant emission. Part 2: computational procedure and parametrical study. *Bull JSME* 1983; 26: 576–583.
- Gao Z and Schreiber W. The effects of EGR and split fuel injections on diesel engine emissions. *Int J Automot Technol* 2001; 2(4): 122–133.
- Morel T and Wahiduzzaman S. Modeling of diesel combustion and emissions. In: *XXVI FISITA Congress*, Prague, Czech Republic, 16–23 June 1996.
- Stiesch G and Merker GP. A phenomenological model for accurate and time efficient prediction of heat release and exhaust emissions in direct-injection diesel engines. SAE paper 1999-01-1535, 1999.
- Aceves SM, Flowers DL, Westbrook CK, Smith JR, Pitz W, Dibble R, et al. A multi-zone model for prediction of HCCI combustion and emissions. SAE paper 2000-01-0327, 2000.
- Babajimopoulos A, Assanis DN, Flowers DL, Aceves SM and Hessel RP. A fully coupled computational fluid dynamics and multi-zone model with detailed chemical kinetics for the simulation of premixed charge compression ignition engines. *Int J Engine Res* 2005; 6(5), 497–512.
- Raju M, Wang M, Dai M, Piggott W and Flowers D. Acceleration of detailed chemical kinetics using multi-zone modeling for CFD in internal combustion engine simulations. SAE paper 2012-01-0135, 2012.
- GT-Power Software, version 7.4, Westmont, IL: Gamma Technologies Inc, <http://www.gtisoft.com/>
- Von Kuensberg Sarre C, Kong SC and Reitz RD. Modeling the effects of injector nozzle geometry on diesel sprays. SAE technical paper series 1999-01-0912, 1999.
- Rezaei R, Eckert P, Seebode J and Behnk K. Zero-dimensional modeling of combustion and heat release rate in DI diesel engines. *SAE Int J Eng* 2012; 5(3): 874–885.
- Weisser GA. Modelling of combustion and nitric oxide formation for medium-speed DI diesel engines: a comparative evaluation of zero- and three-dimensional approaches. PhD Thesis, ETH Zürich, Zürich, 2001.
- Ciezki HK and Adomeit G. Shock-tube investigation of self-ignition of *n*-heptane-air mixtures under engine relevant conditions. *Combust Flame* 1993; 93(4): 421–433.
- Patel A, Kong SC and Reitz RD. Development and validation of a reduced reaction mechanism for HCCI engine simulations. SAE technical paper series no. 2004-01-0558, 2004.
- Kong SC, Han Z and Reitz RD. The development and application of a diesel ignition and combustion model for multidimensional engine simulation. *SAE technical paper series no. 950278*, 1995.

23. Bergeron CA and Hallett WLH. Ignition characteristics of liquid hydrocarbon fuels as single droplets. *Can J Chem Eng* 1989; 67: 142–149.
24. Spalding DB. Mathematical models of turbulent flames; a review. *Combust Sci Technol* 1976; 13: 3–25.
25. Zeldovich YB. The oxidation of nitrogen in combustion and explosions. *Acta Physicochim* 1946; 21: 577–628.
26. Bozzelli JW and Dean AM. O + NNH: a possible new route for NO_x formation in flames. *Int J Chem Kinet* 1995; 27(11): 1097–1109.
27. Bollig M. *Berechnung laminarer Kohlenwasserstoffflammen im Hinblick auf die Stickoxidbildung in Verbrennungsmotoren*. PhD Thesis, RWTH-Aachen University, Aachen, 1998.
28. Smith GP, Golden DM, Frenklach M, Moriarty NW, Mikhail Goldenberg BE, Bowman CT, et al. GRI-Mech 3.0, http://www.me.berkeley.edu/gri_mech/
29. Bowman CT. Kinetics of pollutant formation and destruction in combustion. *Prog Energ Combust* 1975; 1.1: 33–45.
30. Yoshikawa T and Reitz RD. Development of an improved NO_x reaction mechanism for low temperature diesel combustion modeling. SAE technical paper series no. 2008-01-2413, 2008.
31. Vaz AIF and Vicente LN. A particle swarm pattern search method for bound constrained global optimization. *J Global Optim* 2007; 39(2): 197–219.
32. Hadler J, Rudolph F, Dorenkamp R, Stehr H, Hilzenderger J and Kranzusch S. Volkswagen's new 2.0 l TDI engine for the most stringent emission standards—part 1. *MTZ Worldw* 2008; 69(5): 12–18.
33. Greve M. NO_x control with cylinder pressure based engine control systems. *MTZ Ind* 2014; 4(2): 44–53.